SAND2011-5738C

SOFAST FACET CHARACTERIZATION FOR HELIOSTATS: EXTENSIONS AND DIFFICULTIES

Andraka, Charles[1], Yellowhair, Julius[2], Finch, Nolan[2], Ghanbari, Cheryl[2], Chavez, Kyle[2], Sproul, Evan[2]

[1] Sandia National Laboratories, PO 5800 Albuquerque NM USA 87185-1127, (505)844-8573, ceandra@sandia.gov

[2] Sandia National Laboratories, PO 5800 Albuquerque NM USA 87185-1127

Abstract

SOFAST (Sandia Optical Fringe Analysis Slope Tool) uses fringe reflection methods to provide a detailed surface normal map of a reflective facet for CSP systems. SOFAST was developed for point-focus concentrators, and uses a camera and LCD monitor to develop the field of normal vectors. A current need at Sandia is the focusing and characterization of over 5000 heliostat facets as the heliostat field is re-mirrored at the National Solar Thermal Test Facility. The extension of SOFAST to handle nearly-flat facets approximately 1.2m square introduces new sources of uncertainty and new technical challenges. In order to maintain simplicity, we desire methods to characterize the setup without using precision survey equipment.

The modified SOFAST system is in use to focus and characterize the new heliostat facets. The extensions demonstrated in this paper also make SOFAST suitable for trough facet characterization. This paper explains the issues faced during the extension to long focal length facets, and the methods used to solve these issues. A sample heliostat characterization and comparison to field measurements is provided.

1. Introduction

SOFAST (Sandia Optical Fringe Analysis Slope Tool) uses fringe reflection methods to provide a detailed surface normal map of a reflective facet for CSP systems [1]. SOFAST was developed for point-focus concentrators, and uses a camera and LCD monitor to develop the field of facet normal vectors. The fringe reflection method allows a full field characterization (1-2 million pixels) in 10-20 seconds. A reflection of the target LCD screen is viewed in the facet by the camera, while a series of fringe patterns are displayed on the LCD. A simple transformation converts the brightness sequence of each pixel into a screen position on the LCD [2]. Given the camera location, this calculated screen position, and the position of the facet (Figure 1), a surface normal vector can be determined at each location. A recent sensitivity and error analysis [3] indicates excellent accuracy can be attained with this system on point focus facets, when the system is located near the 2f point of the facet.

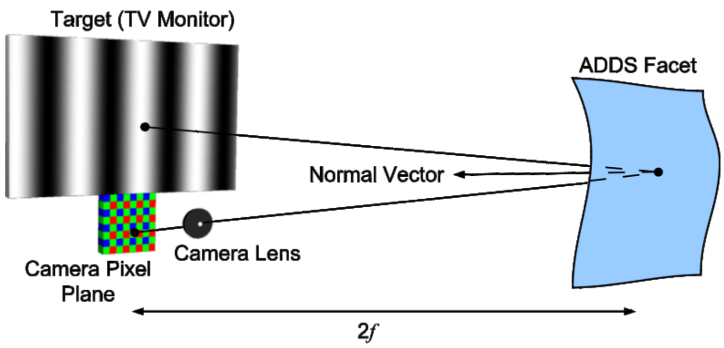

Figure 1. SOFAST physical layout, showing development of the surface normal vector from a representative camera pixel and return location on the target screen.

A current need at Sandia is the focusing and characterization of over 5000 heliostat facets as the field is re-mirrored at the National Solar Thermal Test Facility (NSTTF). Each facet is approximately a 1.2 m square glass mirror (Figure 2), and is supported by a steel ring. Focusing is effected by a pull plate in the center of the facet, providing a single adjustment point. The corners of the facet, outside the ring, were not effectively focused. Therefore, small screw adjusters were added to help shape the four corners. The slant range of the NSTTF heliostat field varies from approximately 50 m to 200 m, so 2-f measurement of the facet shape is not practical.

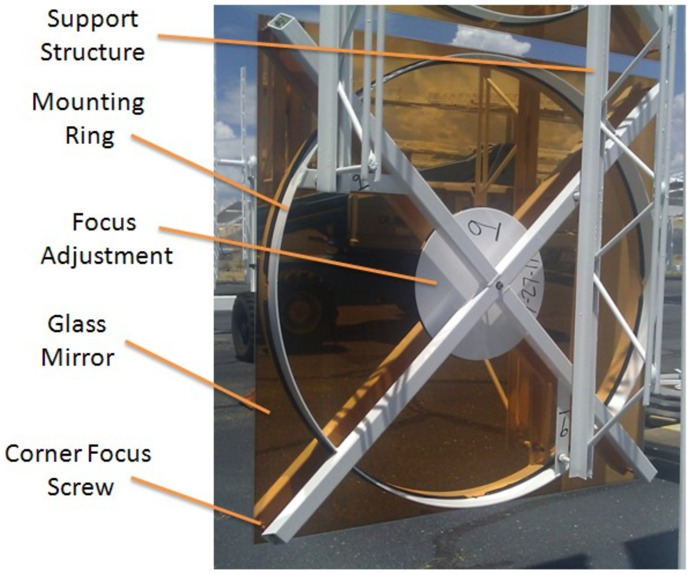

Figure 2. Sandia heliostat facet support structure.

Extension of SOFAST to handle nearly-flat facets introduces new sources of uncertainty and new technical challenges. Primarily, the target screen must be more than twice the size of the facet in each direction, eliminating the use of an LCD monitor. A projection system adds uncertainty and setup difficulties to the screen system, since the pixels are no longer fixed in space. The camera is no longer necessarily perpendicular to the target plane. In order to maintain simplicity and portability to visit customer sites, we desire methods to characterize the setup without using precision survey equipment. CSP trough facets are nearly flat in one direction, and therefore exhibit similar challenges as these heliostat facets.

This paper explains the issues faced during the extension to long focal length facets, and the methods used to solve these issues. Sample heliostat characterization, focusing, and field verification is provided.

2. Background

The point-focus version of SOFAST utilizes a flat LCD monitor as a target surface for the display of fringe patterns. The advantage of the LCD monitor is that the pixels are fixed in a regular grid, and the pixel spacing can be inferred from the overall display dimensions. In addition, the camera can be permanently affixed to the monitor, and easily aligned to be perpendicular to the surface of the monitor.

The nearly-flat facets require a target screen more than twice the size of the facet, to account for the reflected rays from a flat facet plus any errors. Therefore, we chose to use a DLP (LCD) projection system and a 3.6 m square flat white target surface. In such a system, the pixel locations may not be fixed in a regular grid, and must be characterized. The camera is no longer necessarily perpendicular to the screen, and so a rotation vector must be accurately determined. The screen is no longer "black" when a pixel is "off", so we must control and characterize ambient lighting. Finally, since the focal lengths are very long, very small errors in the screen physical layout can result in large errors in the apparent focal length of the facet [4].

While we can determine some of the parameters using high quality surveying equipment, we worked to develop methods that could characterize the system with simple linear measurements and images from the camera. This would allow for simpler deployment of the system to potential partners.

3. SOFAST Setup

3.1. Camera Angle

The camera position relative to the screen center must be known in six degrees of freedom (DOF). The linear measurements can be determined by careful measurement with a standard tape measure or laser distance tool. We have developed the following method for determining the camera roll, pitch, and yaw.

A "crosshair" is displayed on the screen and viewed with the camera as reflected by a flat facet positioned at the facet measuring station, as shown in Figure 3. The horizontal line in the reflected image is then extracted and fitted using edge detection algorithms. The rotation of the fitted line relative to the camera focal plane is calculated to give the relative roll rotation between the camera and the target screen, accounting for the pitch and yaw of the facet relative to the camera and the camera relative to the screen.

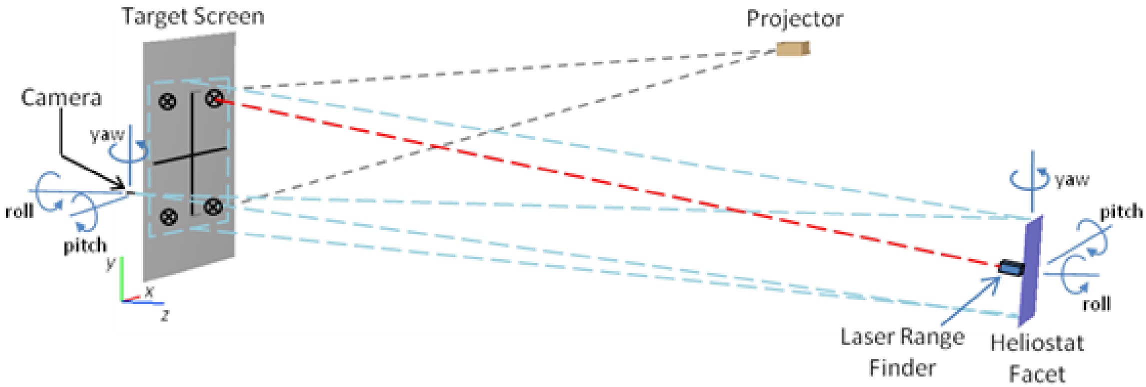

Figure 3. A crosshair display on the target captured in reflection with the camera helps to determine the camera roll relative to the target screen center. Distance measurements determine the pitch and yaw of the camera. Photogrammetric analysis of camera images determine the 6 DOF of the facet relative to the camera.

Multiple laser distance measurements to projected spots on the target screen provide the location of the center of the mirror relative to the screen. The camera position is also measured from the center of the screen. Geometric calculations with these measurements can then determine the pitch and yaw of the camera relative to the screen. The pitch/yaw and roll calculations are interdependent, and the system of equations is solved with a nonlinear solver. An extrinsic analysis of the facet images locates the facet relative to the camera in six DOF, with the camera axis distance trued up by linear measurement. Table 1 lists the angles determined with this tool, compared to those determined with survey equipment. The survey is unable to determine roll.

Table 1. Camera rotation calculations compared to survey.

	Crosshair Method (radians)	From Survey (radians)
Pitch	0.0518	0.0545
Yaw	0.0893	0.0848
Roll	0.0041	N/A

3.2. Screen Pixel Grid

The screen pixel grid can have distortions due to the projector lens, the projector position (keystone), and screen flatness. With long focal length facets, we found the millimeter-scale distortion could impose errors of meters into the apparent focal length [4]. We displayed an 11x11 grid with pixel-wide lines on the screen and carefully measured the grid spacing. This grid is compared to a uniform design grid (Figure 4), and is used to correct for the screen distortions using a 2-D cubic spline interpolation. We found distortions were generally limited to less than 6 mm. We are evaluating photographic techniques for obtaining the measured screen positions, rather than using survey equipment.

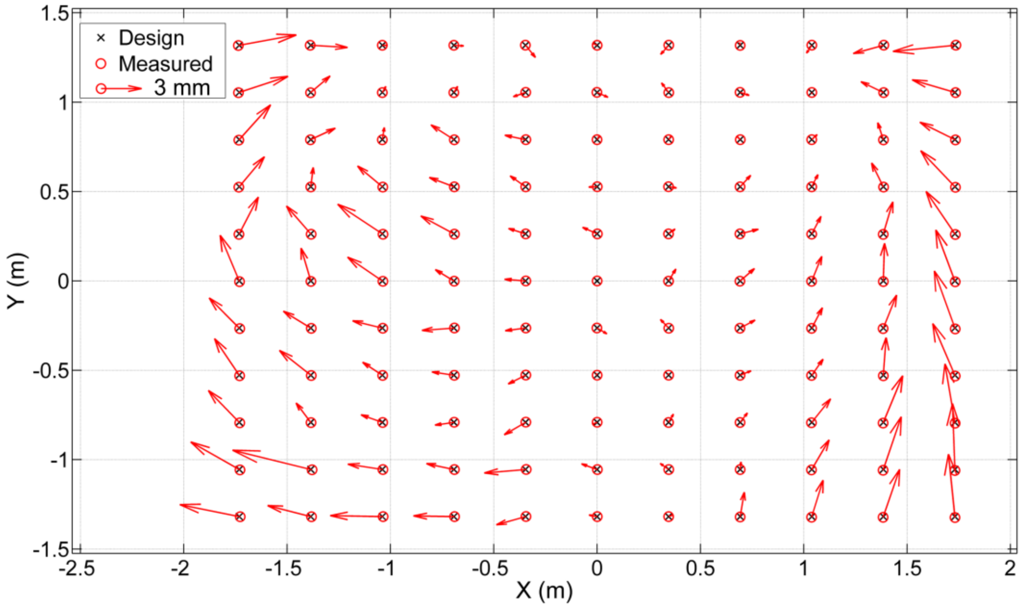

Figure 4. Projector lens distortion. Black x's are design, red points are projected and measured by survey equipment, and red arrows illustrate the magnitude and direction of the difference.

3.3. Screen brightness

We control the lighting during each test, using a canvas tarp "tunnel" to block overhead lighting. We also calibrate the system end-to-end such that the maximum dynamic range of the camera is used. Figure 5 indicates the loss of dynamic range when excessive light is directed to the screen by opening the test bay doors. The doors-closed case still has sufficient ambient lighting for reading or working. We linearize the response of the system end-to-end by adjusting the fringe brightness to eliminate gamma corrections. The camera used reports brightness from 16 to 236, an artifact of YUV encoding.

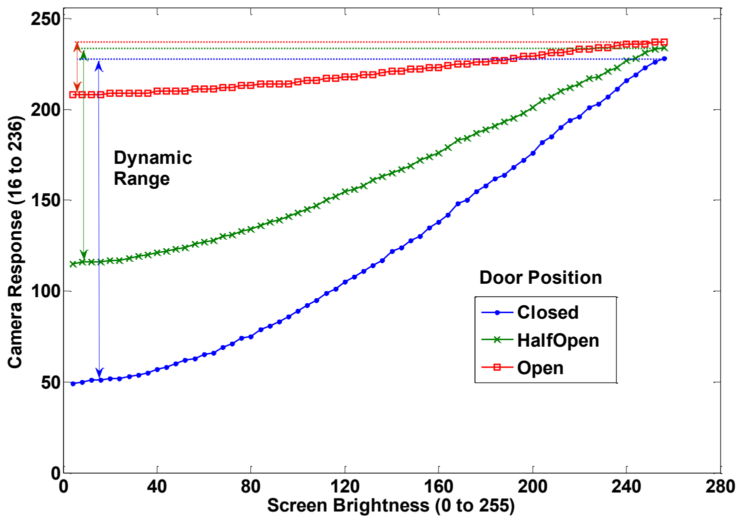

Figure 5. Camera response to screen brightness, reflected in a facet, with varying amounts of background lighting.

3.4. Focus area

Due to the design of the facet support structure, focusing with the middle screw does not impact the corners of the facet. Therefore, we modified SOFAST to report the facet focal length for just the center 1m diameter area of the facet. This area of the facet is focused first, and then the corner adjustments are made independently.

3.4. Verification

We measured several heliostat facets at several rotational orientations to confirm that we had removed systematic target distortions. Rotating the facet 90° confirms the overall global and local aspect ratios, as well as angles, are consistently determined. Figure 6 shows that the facet focal lengths were nearly independent of rotation, for both the full facet and the center 1m focal area. The remaining distortions were traced to support frame distortions when mounted on the test stand.

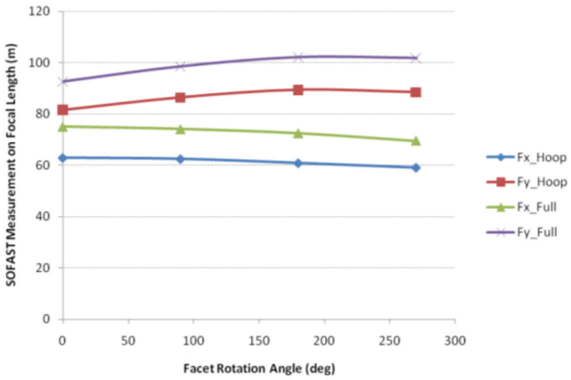

Figure 6. SOFAST-measured facet focal lengths at different facet orientations on the test fixture. The focal length axis is relative to the facet, and so rotates with the facet.

4. Field Results

4.1. Prior Focusing Methods

Prior to the modifications to SOFAST, the new heliostat facets were focused by using a straight edge across the facet and a feeler gauge to set the focus pull. This method provided limited resolution and therefore limited control of spot size on the tower. We also implemented a lookback system, in which a grid of 121 spots was viewed in the reflection of the facet and compared visually to a theoretical overlay of the grid points for a properly focused facet (Figure 7). This method provides a very limited dataset for the facet, and had difficulty accommodating facet distortions and facilitating corner adjustments. Figure 8 shows the spot size after lookback focusing, with the facet at design (b, 55m), and offset from design by -/+ 13m (a/c). The spot size and shape is less than ideal. Some of the flare seen in the image is due to distortion along the lower edge of the mirror, which can be seen in Figure 7.

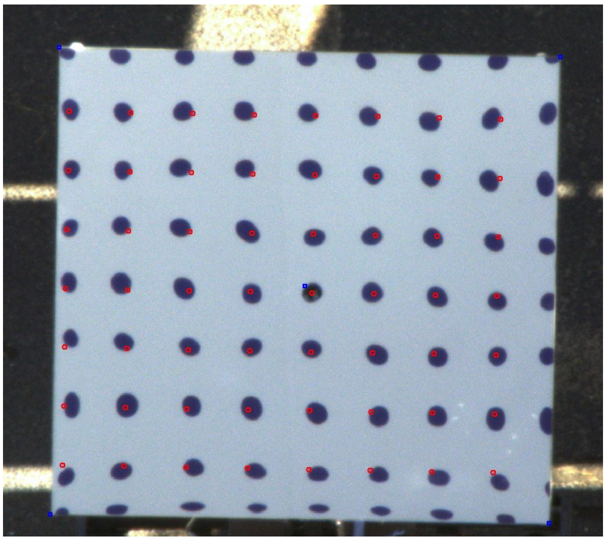

Figure 7. Dot lookback focusing method with theoretical dot position overlay.

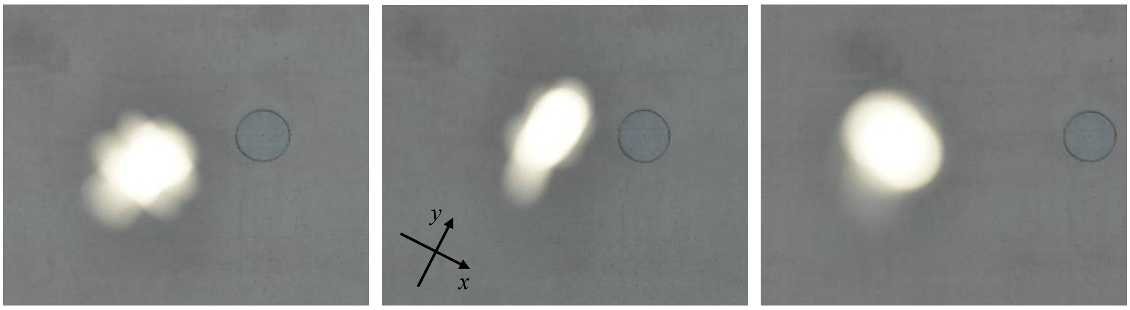

(a) **(b)** **(c)**

Figure 8. Beam image of dot-lookback focused facet with 55m slant range. (b) Facet at the 55 m slant range, and at positions (a) one heliostat row forward and (c) one heliostat row back.

4.2. SOFAST Focusing

When characterizing the facets with SOFAST, we found that the glass was not strictly flat, but had residual distortions. In particular, most glass pieces tested have a slight bend along one edge (bottom of facet in Figure 9), as well as an astigmatism. SOFAST reports a different focal length in the X and Y directions (astigmatism). The facet imaged in Figure 9, after focusing with SOFAST feedback, has focal lengths of 116m in the horizontal direction and 190m in the vertical direction, considering only the center 1m diameter. Through experimentation, we found that focusing the shorter focal length provided the smallest spot size on the tower target. This agrees with the first-order equations presented by Igel and Hughes [5]. Thus, we determined to set the shorter focal length to the slant range for each row of heliostats.

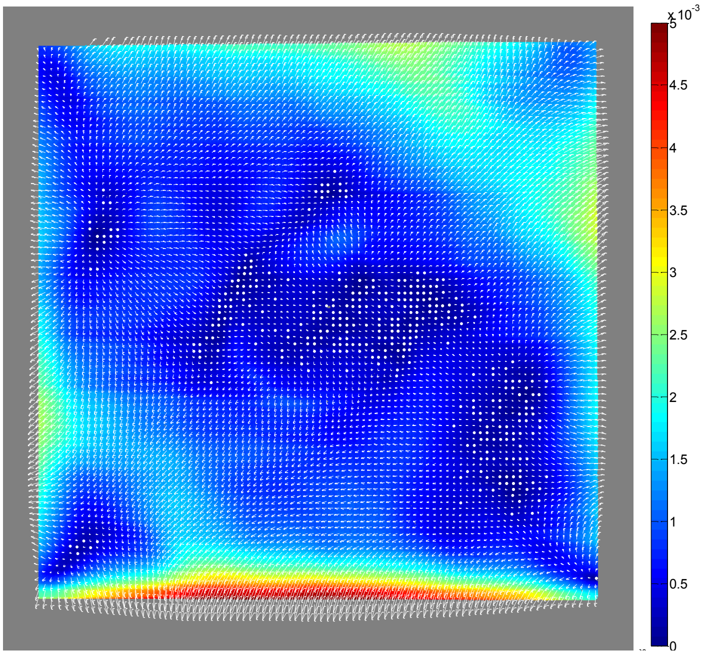

Figure 9. SOFAST characterization of selected heliostat facet. The color indicates the magnitude of the slope error, and the vectors indicate direction trends. The slope error is relative to a design 115m focal length facet.

The same facet tested in Figure 9 was the placed in the field near solar noon and the spot size on the tower imaged. We moved the facet incrementally away from the tower in roughly 6m slant range steps, with the spot images presented in Figure 10. The best apparent spot shape and size coincides with the measured short focal length of 116m. In addition, since the corners are focused, the spot shape looks considerably better than the lookback-focused facet in Figure 8. The slight smear of light below the image is caused by the bent edge of the heliostat facet.

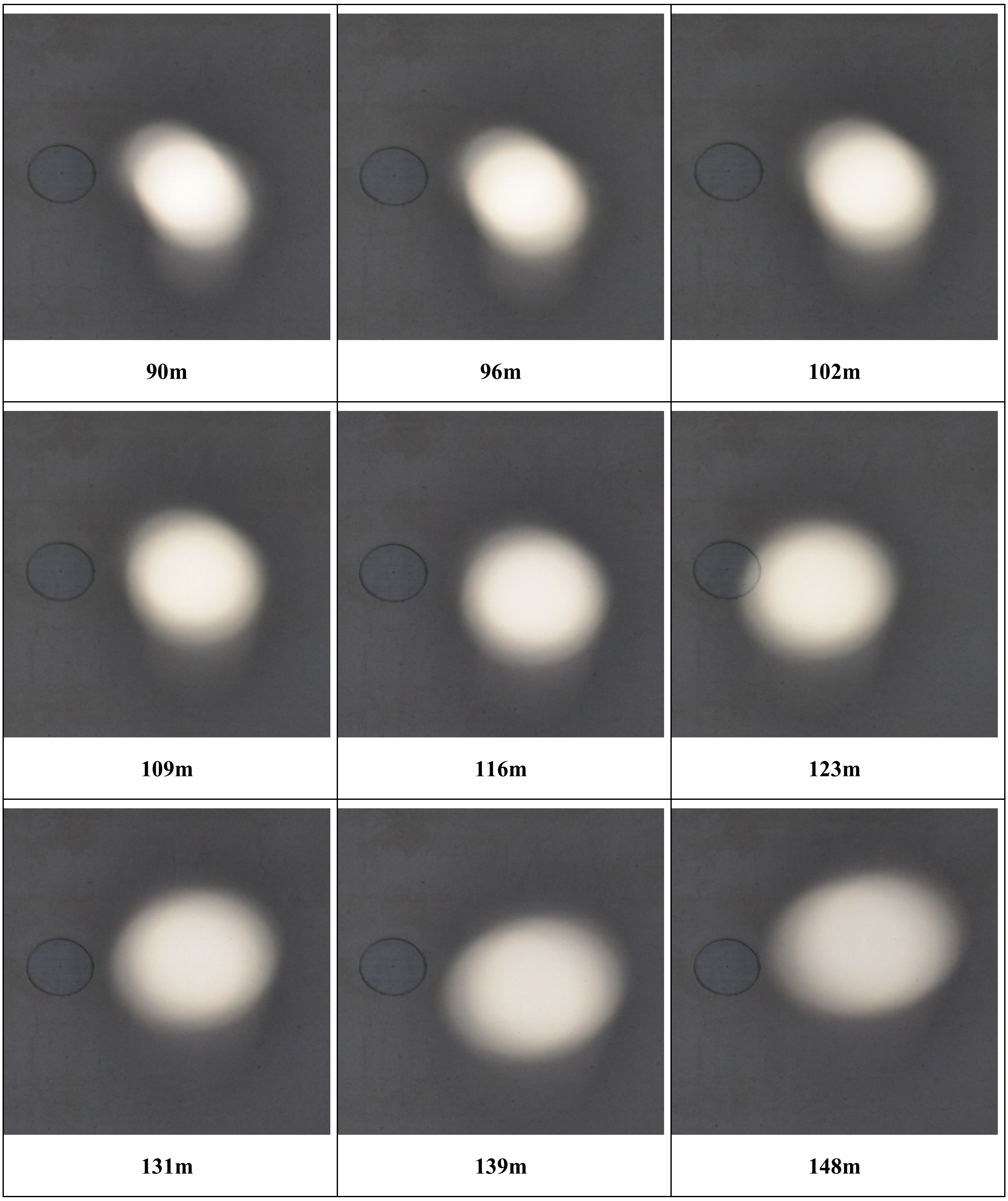

Figure 10. Tower spot images from SOFAST-focused facet. The short focal length of the facet is set to 116m.

4.3. Full Heliostat Comparison

Figure 11 shows flux profiles from two adjacent heliostats captured with the beam characterization system (BCS) at the same time of day. The slant range of the two heliostats (5 × 5 facets) to the tower wall is 115 m. For the first heliostat (Figure 11a), the 25 facets were focused with the depth gauge. The facets on the second heliostat (Figure 11b) were focused with SOFAST. The flux profiles show that the heliostats with facets focused with SOFAST show a higher peak flux (75-80 a.u.) than the heliostat with facets focused with the depth gauge (65-70 a.u.).

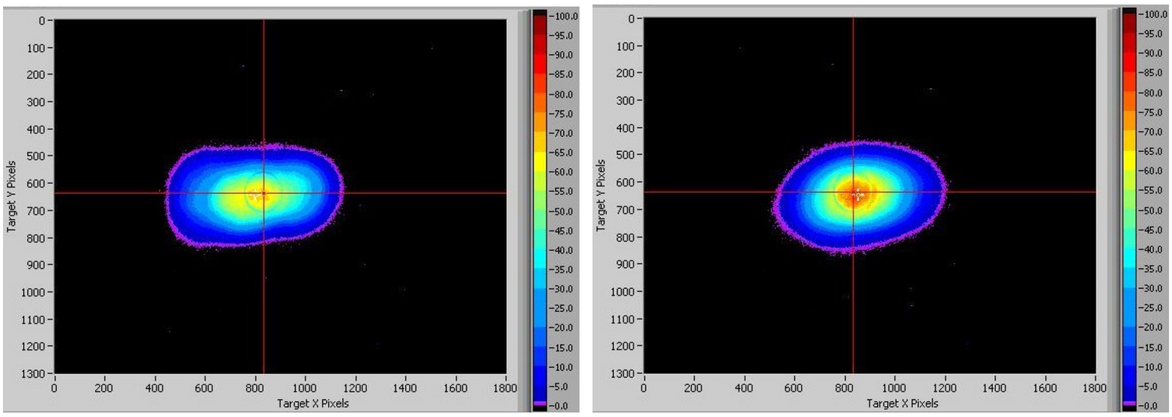

(a) **(b)**

Figure 11. Flux captured with the BCS (61.5 pix/m) from two adjacent heliostats with the facets focused with a) a depth gauge and b) SOFAST. The heliostats are adjacent to each other and have a slant range of about 115 m.

5. Conclusion

We have successfully extended SOFAST to characterize nearly-flat facets, and implemented the revised system to focus heliostats for Sandia's refurbished field. The modifications to SOFAST include a large projection screen for display of fringe patterns. The setup of SOFAST must take into account the screen non-uniformities, the camera rotation angles, and the ambient lighting. Measures were developed to address these issues in a laboratory setting.

Field testing of SOFAST-focused facets demonstrates a better focused spot, in terms of size and peak brightness, than prior less analytical methods employed. The Heliostat version of SOFAST will be used to focus facets for the refurbished field installation.

Acknowledgements

This manuscript has been authored by Sandia Corporation under Contract No. DE-AC04-94AL85000 with the U.S. Department of Energy. The United States Government retains and the publisher, by accepting the article for publication, acknowledges that the United States Government retains a non-exclusive, paid-up, irrevocable, world-wide license to publish or reproduce the published form of this manuscript, or allow others to do so, for United States Government purposes.

References

[1] Andraka, C.E., Sadlon, S., Myer, B, Trapeznikov, K., Liebner, C. (2009), "Rapid Reflective Facet Characterization Using Fringe Reflection Techniques", *Proceedings of Energy Sustainability 2009*, ASME, San Francisco, CA USA, July 19-23.

[2] Bothe, T., Li, W., von Kopylow, C., Jüptner, W., (2004), "High Resolution 3D Shape Measurement on Specular Surfaces by Fringe Reflection", *Optical Metrology in Production Engineering, Proceedings of SPIE* Vol. 5457, Bellingham, WA. USA

[3] Finch, N.S., and Andraka, C.E. (2011), "Uncertainty Analysis and Characterization of the SOFAST Mirror Facet Characterization System", *Proceedings of Energy Sustainability 2011*, ASME, Washington DC, USA, August 7-10.

[4] Yellowhair, J., Andraka, C.E., and Finch, N.S., (2011), "Heliostat Focal Length Impacts on SOFAST Sensitivity", *Proceedings of Solar Paces 2011,* Solar Paces, Granada Spain, September 20-23.

[5] Igel, E.A., and Hughes, R.L., (1979), "Optical Analysis of Solar Facility Heliostats", *Solar Energy,* Volume 22, Issue 3, pp. 283-295.